

First identification, chemical analysis and pharmacological characterization of *N*-piperidinyl etonitazene (etonitazepipne), a recent addition to the 2-benzylbenzimidazole opioid subclass

Marthe M. Vandeputte^{1,#}, Nick Verougstraete^{1,2,#}, Donna Walther³, Grant C. Glatfelter³, Jeroen Malfliet⁴, Michael H. Baumann³, Alain G. Verstraete^{2,5}, Christophe P. Stove^{1,*}

¹ Laboratory of Toxicology, Department of Bioanalysis, Faculty of Pharmaceutical Sciences, Ghent University, Ghent, Belgium

² Department of Laboratory Medicine, Ghent University Hospital, Ghent, Belgium

³ Designer Drug Research Unit, Intramural Research Program, National Institute on Drug Abuse, National Institutes of Health, Baltimore, MD 21224, USA

⁴ Huisartsenpraktijk De Leeuwerik, Dendermonde, Belgium

⁵ Department of Diagnostic Sciences, Ghent University, Ghent, Belgium

These authors contributed equally to this work.

* Corresponding author: christophe.stove@ugent.be

Abstract (250 words)

N-piperidinyl etonitazene ('etonitazepipne') represents a recent addition to the rapidly expanding class of 2-benzylbenzimidazole 'nitazene' opioids. Following its first identification in an online-sourced powder and in biological samples from a patient seeking help for detoxification, this report details its in-depth chemical analysis and pharmacological characterization. Analysis of the powder via different techniques (LC-HRMS, GC-MS, UHPLC-DAD, FT-IR) led to the unequivocal identification of *N*-piperidinyl etonitazene. Furthermore, we report the first activity-based detection and analytical identification of *N*-piperidinyl etonitazene in authentic samples. LC-HRMS analysis revealed concentrations of 1.21 ng/mL in serum and 0.51 ng/mL in urine, whereas molecular networking enabled the tentative identification of various (potentially active) urinary metabolites. In addition, we determined that the extent of opioid activity present in the patient's serum was equivalent to the *in vitro* opioid activity exerted by 2.5-10 ng/mL fentanyl or 10-25 ng/mL hydromorphone in serum. Radioligand binding assays in rat brain tissue revealed that the drug binds with high affinity ($K_i=14.3$ nM) to the μ -opioid receptor (MOR). Using a MOR- β -arrestin2 activation assay, we found that *N*-piperidinyl etonitazene is highly potent ($EC_{50}=2.49$ nM) and efficacious ($E_{max}=183\%$ versus hydromorphone) *in vitro*. Pharmacodynamic evaluation in male Sprague Dawley rats showed that *N*-piperidinyl etonitazene induces opioid-like antinociceptive, cataleptic, and thermic effects, its potency in the hot plate assay ($ED_{50}=0.0205$ mg/kg) being comparable to that of fentanyl ($ED_{50}=0.0209$ mg/kg), and >190 times higher than that of morphine ($ED_{50}=3.940$ mg/kg). Taken together, our findings indicate that *N*-piperidinyl etonitazene is a potent opioid with the potential to cause harm in users.

1. Introduction

The number of new synthetic opioids (NSOs) appearing on the recreational drug market continues to increase. While raising concern due to their role in the current phase of the opioid epidemic in the United States (U.S.) (Ciccarone 2019; UNODC 2020), NSOs are also increasingly detected in Europe. A total of 73 different NSOs has been formally notified to the EU Early Warning System (EWS) on new psychoactive substances (NPS) between 2009 and 2021, with more than half being reported in the last 4 years (EMCDDA 2021). While newly emerging opioids present with progressively diverse chemical structures (UNODC 2020), opioids with a 2-benzylbenzimidazole core have recently become increasingly prevalent (Ujváry et al. 2021; Vandeputte et al. 2021b; Walton et al. 2021).

2-Benzylbenzimidazole opioids, also referred to as 'nitazenes', originate from a series of research articles published in the late 1950s, when this structural scaffold was explored for its analgesic effects by the pharmaceutical company CIBA. In mouse studies, several members of this group of analgesics showed levels of antinociceptive potency several orders of magnitude higher than that of morphine (Gross and Turrian 1957; Hunger et al. 1957, 1960a, b, c; Ujváry et al. 2021). While promising in terms of their antinociceptive effects, none of these substances were ever further developed into medicines, likely due to a high risk of adverse events (Bromig 1958; EMCDDA 2020; Ujváry et al. 2021). As with many failed pharmaceuticals researched in the second half of the twentieth century, 2-benzylbenzimidazole opioids were recently 're-discovered' by clandestine drug manufacturers and subsequently introduced onto the recreational drug market (Sharma et al. 2019; UNODC 2020). Between 1966 and 2003, the only 2-benzylbenzimidazole 'nitazene' opioid that was sporadically identified in the illicit drug supply was etonitazene (Brandenberger 1974; Sorokin 1999; Sorokin et al. 1999; Reavy 2003; Morris 2009; EMCDDA 2020), a harmful opioid described to be 1000 times more potent than morphine in a rodent model of antinociception (Gross and Turrian 1957; Hunger et al. 1960b). However, it was the emergence of isotonitazene in 2019 that really sparked the rapid expansion of 2-benzylbenzimidazole opioids on the recreational drug market. Quickly after its first emergence, the popularity of isotonitazene among NPS opioid users started rising, until the drug dominated the NPS opioid market in the first half of 2020 (Vandeputte et al. 2021a). By now, isotonitazene has decreased in popularity, in part following the introduction of

several legislative restrictions (Vandeputte et al. 2021a) and finally its international scheduling in June 2021 (UNODC 2021). Demonstrating the dangers of this class of NPS opioids, isotonitazene has been associated with over 250 deaths in the U.S. (Krotulski et al. 2020). After isotonitazene positivity began to wane, different other ‘nitazene’ analogues appeared on recreational drug markets worldwide (**Figure 1**).

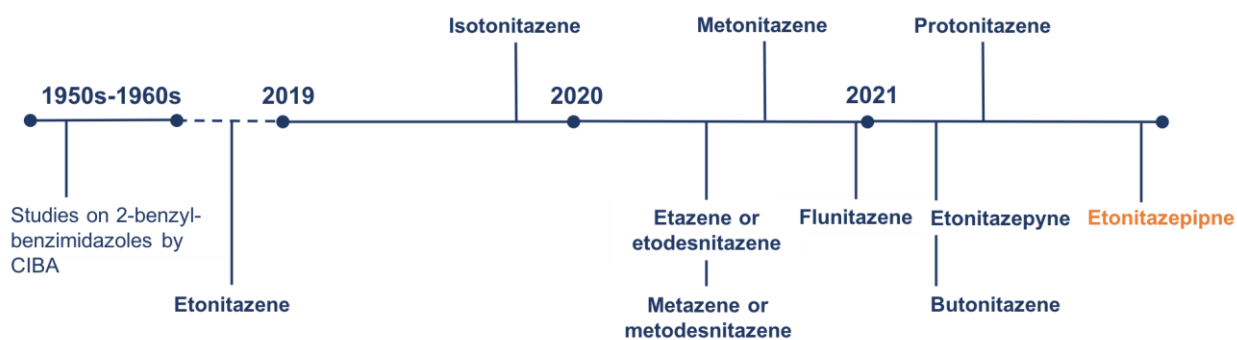


Figure 1. Timeline of the emergence of 2-benzylbenzimidazoles on the recreational drug market. Etonitazene has been sporadically identified between 1966 and 2003. Data for other nitazenes indicate first formal notification to the EU Early Warning System on new psychoactive substances (EMCDDA).

Previously, we investigated the μ -opioid receptor (MOR) activation potential of all 2-benzylbenzimidazoles that have been identified on the recreational drug market (Vandeputte et al. 2021b) (Vandeputte & Krotulski *et al.*, in press). Our results showed that these compounds are generally highly active agonists, with potencies and efficacies of several analogues exceeding those of fentanyl and morphine. Here, we report on a further expansion of the group of nitazenes, with the first identification of *N*-piperidinyl etonitazene (‘etonitazepipne’) in early November 2021. That same month, a biological sample in the U.S. tested positive for this compound (Krotulski et al. 2021a). Early research on this opioid revealed an antinociceptive potency exceeding that of morphine (Hunger et al. 1960b). Here, we report on the full chemical and pharmacological characterization of *N*-piperidinyl etonitazene and its first identification in Europe. The drug was sourced online and used by a patient seeking help for detoxification. In addition to the unequivocal identification and quantification of the parent drug in serum and urine samples from this patient, metabolites were also identified. Furthermore, a cell-based bioassay was used to determine the extent of MOR activation exerted by *N*-piperidinyl etonitazene (and its active metabolites) in the patient samples and in the obtained powder. Last, to further deepen the pharmacological

characterization of this drug, MOR binding affinity and *in vivo* effects (in rats) of *N*-piperidinyl etonitazene were studied.

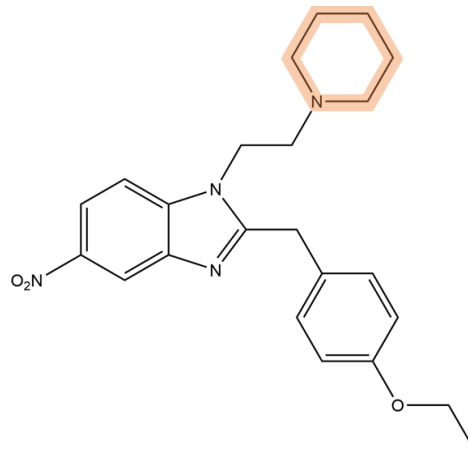


Figure 2. Structure of *N*-piperidinyl etonitazene, colloquially referred to as etonitazepipne.

Case

A 25-year-old man visited his general practitioner with generalized muscle pain and severe abdominal pain including nausea, cramping and diarrhea, asking help for detoxification. The patient had a medical history of generalized anxiety disorder and panic attacks for which he had been treated with escitalopram and alprazolam. At the time of consultation, the patient was not on prescribed (chronic) medications. The patient stated that his current complaints were the result of the use of high doses of *N*-piperidinyl etonitazene, a substance he had been taking for four months (**Figure 3**). He mentioned that his drug use had a negative effect on his health and work life. The patient also admitted the use of several benzodiazepines, including the NPS benzodiazepines etizolam and clonazolam, since 2017. He purchased these different substances either online or via a contact person in his social circle. He initially started taking these drugs because he felt it resulted in a positive effect on his concentration, feeling more sociable and less stressed, unlike the effects of the antidepressants his general practitioner had prescribed in the past.

His use of *N*-piperidinyl etonitazene started when he was suffering from lower back pain. *N*-piperidinyl etonitazene was dissolved in water with citric acid to obtain a nasal solution. After repeated intranasal administration (1 spray equaling approximately 100 µg), he acquired a high tolerance for the substance. His peak use was 60 nasal sprays (approximately 6 mg) per day, which quickly resulted in a negligible effect on his pain complaints. In this period his drug use derailed to a moment where he ate a fentanyl patch (75 µg/h), in search for a high. His

benzodiazepine misuse was still ongoing at this time and the patient stated his functioning was getting more and more dependent on his growing medication intake. He reported no use of alcohol or other medications/drugs.

After consultation with his general practitioner, the patient was referred to an outpatient rehabilitation center where his *N*-piperidinyl etonitazene use was gradually reduced to zero. He was still in treatment for detoxifying from his benzodiazepines misuse. Written informed consent was obtained from the patient.

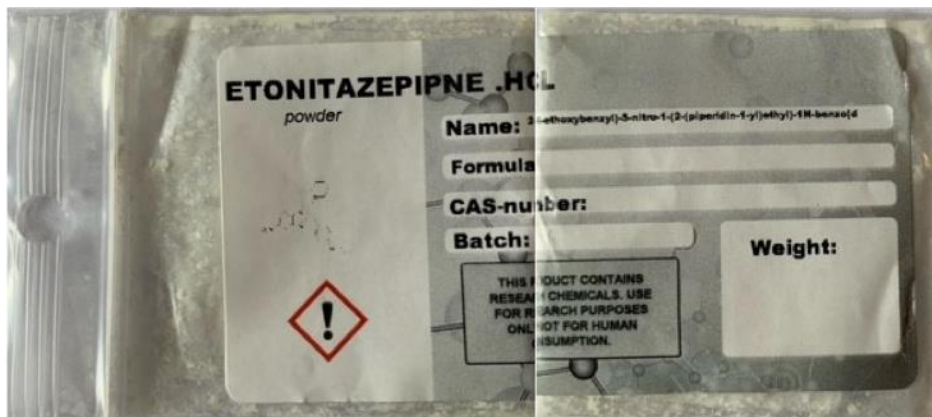


Figure 3. Picture of the obtained online-sourced powder sachet containing *N*-piperidinyl etonitazene. The label was folded around the sachet and contained the name and structure of the compound, together with warnings typically found on NPS packaging (e.g. ‘this product contains research chemicals’, ‘use for research purposes only’, ‘not for human consumption’).

2. Methods

2.1 Materials

The reference standards for *N*-piperidinyl etonitazene, morphine and fentanyl were obtained as neat powders from Cayman Chemical (Ann Arbor, Michigan, U.S.). Etonitazene (1 mg/mL in acetonitrile (ACN)) was purchased from Chiron AS (Trondheim, Norway). Hydromorphone powder was from Fagron (Nazareth, Belgium) and trimipramine-D₃ from Cerilliant (Round Rock, TX, U.S.). Morphine sulfate (morphine) and fentanyl citrate (fentanyl) for radioligand binding assays and *in vivo* studies were generously provided by the National Institute on Drug Abuse (NIDA) Drug Supply Program (NDSP, Rockville, MD, U.S.), and the results of these experiments with morphine and fentanyl were also used in Vandeputte & Krotulski *et al.* (in press). Formic acid (FA), methanol (MeOH) and ACN were all LC-MS grade and obtained from Biosolve (Dieuze, France). Dimethyl sulfoxide (DMSO) was purchased from Fluka (Charlotte, NC, U.S.). Ammonium formate was from Sigma-Aldrich (Saint Louis, MI, U.S.) and abalonnase (purified β -glucuronidase) was from Ango (San Ramon, CA, U.S.). Dulbecco's Modified Eagle's Medium (DMEM, supplemented with GlutaMAX[®]), Opti-MEM[®] I Reduced Serum Medium, penicillin/streptomycin (10000 IU/mL and 10000 μ g/mL), and amphotericin B (250 μ g/mL) were purchased from Thermo Fisher Scientific (Pittsburgh, PA, U.S.). Promega (Madison, Wisconsin, U.S.) supplied the Nano-Glo Live Cell Reagent and the Nano-Glo LCS Dilution Buffer. Fetal Bovine Serum (FBS) and poly-D-lysine were obtained from Sigma-Aldrich (Overijse, Belgium).

2.2 Calibrators and QCs for LC-HRMS quantification

A stock solution of *N*-piperidinyl etonitazene (Cayman reference standard) was prepared in DMSO at a concentration of 6.80 mg/mL and further diluted in DMSO to obtain working solutions. Calibrators were prepared at six concentrations by spiking working solutions to blank calf serum at concentrations of 0.5, 1.0, 2.5, 5.0, 10 and 20 ng/mL or to blank human urine from a healthy volunteer at concentrations of 0.25, 0.5, 1.25, 2.5, 5.0 and 10 ng/mL. Quality control (QC) samples (lower limit of quantification (LLOQ), medium and high) were prepared by spiking different working solutions to blank calf serum at 0.5, 3.0 and 15 ng/mL and to blank human urine at 0.25, 1.0 and 8.0 ng/mL. Calibrators and QC samples were aliquoted and stored at -20°C until analysis.

2.3 Description of the powder and sample preparation

A transparent plastic bag labeled 'etonitazepipne HCl' (**Figure 3**) was obtained from the patient, who had purchased this powder from an online vendor. The label stated "This product contains research chemicals, use for research purposes only. Not for human consumption.". The bag contained a remainder of a white-yellowish powder of which 10 mg was dissolved in 10 mL MeOH, resulting in a stock solution of 0.918 mg/mL, considering that the label stated it was a HCl salt. This solution (stored at -20°C) was used for assessing biological activity and for chromatographic analyses. For the latter, the stock solution was further diluted in water to 92 µg/mL for gas chromatography-mass spectrometry (GC-MS) and ultra-high-performance liquid chromatography-diode array detector (UHPLC-DAD) analysis, and to 9.2 µg/mL for liquid chromatography high-resolution mass spectrometry (LC-HRMS) screening analysis.

2.4 Patient samples

One serum and one urine sample, collected at the same time upon first presentation of the patient, were available for toxicological analysis. For LC-HRMS screening and quantitative *N*-piperidinyl etonitazene analysis, 50 µL sample (either serum or urine) and 50 µL of internal standard solution (given that no *N*-piperidinyl etonitazene isotope-labeled standard was available, trimipramine-D₃ 500 ng/mL was used in water as routinely applied in our lab) were mixed. After addition of 200 µL cold MeOH/ACN (50/50) or 200 µL mobile phase A (2 mM ammonium formate, 0.1% formic acid (FA)) to respectively serum and urine samples, samples were shaken for 5 minutes at 1400 rpm and 5°C. Next, the samples were centrifuged for 5 minutes at 16,162 g. Fifty µL of the supernatant was transferred to vials, and 5 µL (for serum) or 20 µL (for urine analysis) were injected onto the UHPLC column (cfr. infra).

For the MOR activation bioassay, 200 µL of serum or urine was mixed with 800 µL methanol/acetonitrile (50/50) and 200 µL water (rather than internal standard solution). After shaking and centrifugation (20,800 g), the supernatant was transferred to a glass tube and evaporated at 40°C under a gentle stream of nitrogen (Turbovap[®] LV, Biotage, Uppsala, Sweden). Once dry, the extracts were reconstituted in 100 µL Opti-MEM I, and 20 µL was used in the bioassay.

For semi-quantification of *N*-piperidinyl etonitazene in serum and urine using the bioassay, a standard addition approach was followed. For this purpose, aliquots of the patient samples

were fortified with 1.5 ng/mL of *N*-piperidinyl etonitazene and the resulting extracts were run in parallel with extracts from non-fortified patient serum or urine samples.

For determination of fentanyl and hydromorphone 'MOR activity-equivalents', bovine serum extracts were spiked with different concentrations of fentanyl (0.1-25 ng/mL), hydromorphone (1-75 ng/mL) or *N*-piperidinyl etonitazene (1 ng/mL), the latter as a substitute for the patient serum sample to avoid potential effects of matrix differences between bovine and human serum. Potential differences in recovery between the three analytes were eliminated by spiking the extracts (post-processing of the sample) rather than the blank bovine serum.

2.5 LC-HRMS analysis

The powder and patient samples were analyzed with the same LC-HRMS screening method as described previously (Verougstraete et al. 2020). In brief, chromatographic separation was achieved on an Ultimate 3000 UHPLC system (Thermo Fisher Scientific, Waltham, MA, U.S.) using an Accucore phenylhexyl column (100 mm length x 2.1 mm i.d., 2.6 μ m particle size) combined with gradient elution. The HRMS system was a Q Exactive (Thermo Fisher Scientific) with a full scan range of 70-1000 m/z and resolution of 35,000 (full width at half maximum (FWHM)). Data-dependent acquisition (DDA) was used for screening: high-energy collisional dissociation was performed on maximum five compounds that matched the inclusion list. If there were less than five ions matching the inclusion list, the most intense precursor ions were also fragmented.

On the same Q Exactive system a HR accurate mass detection method was developed for the quantification of *N*-piperidinyl etonitazene in the patient samples using targeted selected ion monitoring. The exact monoisotopic mass for *N*-piperidinyl etonitazene was 409.2234 m/z and for trimipramine- D_3 298.2357 m/z with a measuring window set at 5 ppm and a mass resolution of 70,000 FWHM. The automatic gain control (AGC) was set at $1e6$ and the maximum injection time at 200 msec. The same UHPLC column and mobile phases as for the screening method were used. The total run time was 8 min. A fit-for-purpose validation was performed. Calibration curves were linear (weighted $1/x^2$) between 0.5 and 20 ng/mL and between 0.25 and 10 ng/mL for serum and urine, respectively. Using this selected model, the bias on back-calculation of all calibrators was below 14.4%. Within- and between-run ($n = 5$ and 6, respectively) precision over all QC levels (including LLOQ) were $\leq 15.8\%$ and $\leq 18.8\%$ for

respectively serum and urine. Within- and between-run biases in serum and urine were ≤ 7.60 and $\leq 11.4\%$, respectively. A standard addition experiment was performed to exclude the presence of matrix effects or matrix-dependent recoveries. The same concentration of *N*-piperidinyl etonitazene was added to 0.5 (for urine) or 1.0 (for serum) ng/mL QC samples, which were prepared from the same blank matrix as the calibrators, and to the patient urine and serum samples. The increase in response (internal standard corrected) was similar in both the QCs and the patient samples (within 3.6%), showing that the standards and patient samples behave similar in terms of matrix effects and recovery. Lastly, the analysis of six blank samples did not yield interfering peaks within the respective retention times of *N*-piperidinyl etonitazene.

2.6 Tentative metabolite identification

The *in vivo* metabolism of *N*-piperidinyl etonitazene was examined through analysis of the urine and serum sample of the patient. Both samples were prepared as described above. Moreover, the urine sample was also analyzed after β -glucuronidase treatment: a mixture of 10 μ L sample, 10 μ L abalonnase and 10 μ L internal standard solution was incubated for 30 minutes at 37°C after which it was injected onto the UHPLC column. Obtained MS² data from the patient samples were first processed with MZmine2 software (Pluskal et al. 2010), after which the data were analyzed via a Feature-Based Molecular Networking (FBMN) workflow (Nothias et al. 2020) on the Global Natural Products Social Molecular Networking (GNPS) software (Wang et al. 2016). Precursor and MS² fragment ion mass tolerances were set at 0.05 Da. A molecular network was created by including precursor ion masses as nodes to have a cosine score above 0.70 and more than 6 matched peaks. Two nodes should be in each other's respective top 10 of most similar nodes. The maximum size of a molecular network was set at 100.

2.7 GC-MS, UHPLC-DAD and FT-IR analysis

The GC-MS, UHPLC-DAD and Fourier-transform infrared (FT-IR) spectra of the *N*-piperidinyl etonitazene powder were determined as previously described (Verougstraete et al. 2020). In short, a diluted stock of the powder was injected on a GC-2010 system coupled with a GC-MS QP2010 Plus mass spectrometer (Shimadzu, Kyoto, Japan) operated in scanning mode with a scanning range of 40-550 *m/z* and an ionization energy of 70 eV. The DAD spectrum was

obtained by analyzing the powder on an Acquity UPLC™ system with PDA detector (Waters, Milford, MA, U.S.), monitoring wavelengths between 190 and 400 nm with a slit of 0.5 μm and resolution of 1.2 nm. Lastly, the IR spectrum was obtained by depositing a small amount of the powder on the crystal of a Spectrum 2 photometer (Perkin Elmer, Waltham, MA, U.S.) and recording the spectrum in the range of 4000-400 cm⁻¹ with a spectral resolution of 4 cm⁻¹.

2.8 Radioligand binding

To determine the MOR affinities of *N*-piperidinyl etonitazene and reference compounds, radioligand binding assays were carried out as previously described (Truver et al. 2020), with some modifications. Whole rat brains minus cerebellum were purchased from a commercial vendor (BioIVT, Westbury, NY, U.S.). After thawing on ice, membranes were prepared by homogenizing 0.5 g of brain tissue in 20 mL of ice-cold 50 mM Tris HCl (pH 7.4) using a Kinematica Polytron (setting 6 for 20 sec). Homogenates were centrifuged at 19,000 rpm for 15 min at 4° C. Supernatants were discarded, and the pellets were resuspended in fresh buffer and spun again at 19,000 rpm for 15 min. The resulting pellet was then resuspended to yield 100 mg wet tissue weight per mL of buffer. Ligand binding experiments were conducted in polypropylene tubes containing 300 μL Tris buffer and 100 μL of tissue suspension for 60 min at room temperature. The radioligand [³H]DAMGO (Perkin Elmer Life Sciences, Waltham, MA, U.S.) was used at a final concentration of 1 nM to label MOR. Non-specific binding was determined in the presence of 10 μM naloxone. Stock solutions of 10 mM morphine, fentanyl, and *N*-piperidinyl etonitazene were prepared in 100% DMSO and stored at -80°C. Immediately prior to an experiment, aliquots of stock solution were diluted in 50 mM Tris buffer to yield the appropriate concentrations. The binding reaction was terminated by rapid vacuum filtration through Whatman GF/B filters (Whatman Inc., Clifton, NJ, U.S.) using a cell harvester (Brandel Instruments, Gaithersburg, MD, U.S.). Filters were washed three times with Tris buffer and transferred to 24-well plates before addition of Cytoscint (MP Biomedicals, Irvine, CA, U.S.). The next day, a Perkin Elmer MicroBeta2 liquid scintillation counter was used to count radioactivity. Raw cpm data were normalized to percent of radioligand bound, and K_i values were determined using nonlinear regression analysis using GraphPad Prism 8.2 software (San Diego, CA, U.S.).

2.9 μ-Opioid receptor (MOR) activation assay

Assay protocol

A previously reported cell-based MOR activation assay (Cannaert et al. 2019; Vasudevan et al. 2020) was used to determine the MOR agonistic activity of the *N*-piperidinyl etonitazene reference standard and the obtained powder, as well as the opioid activity present in the patient samples (serum and urine). The assay monitors MOR activation via recruitment of β -arrestin 2 (β arr2) (coexpressed with G protein-coupled receptor kinase 2, GRK2) using the NanoLuc Binary Technology[®] (Promega). In short, activation of MOR, fused to one part of a split nanoluciferase enzyme, leads to recruitment of β arr2, fused to the complementing subunit. This leads to functional complementation of the split nanoluciferase. Upon addition of the substrate furimazine, a measurable bioluminescent signal is generated.

Human embryonic kidney (HEK) 293T cells stably expressing the MOR- β arr2-GRK2 system were routinely cultured in DMEM (Glutamax[®], supplemented with 10% heat-inactivated FBS, 100 IU/mL penicillin, 100 mg/L streptomycin and 0.25 mg/L amphotericin B) at 37°C in a humidified atmosphere containing 5% CO₂. The stability of the cell line was monitored on a regular basis via flow cytometric analysis of co-expressed markers (Vasudevan et al. 2020). On day one of the assay protocol, the cells were seeded on white, poly-D-lysine pre-coated 96-well plates (5 x 10⁴ cells/well). After overnight incubation, the cells were washed twice with Opti-MEM[®] I reduced serum medium, before addition of 90 μ L Opti-MEM[®] to each well. Nano-Glo Live Cell Reagent was subsequently prepared by 20-fold dilution of Nano-Glo Live Cell Substrate with Nano-Glo LCS Dilution Buffer, and 25 μ L was added to the cells. The plate was then placed into a Tristar² LB 942 microplate reader (Berthold Technologies GmbH & Co., Bad Wildbad, Germany), and luminescence was continuously monitored until a stable signal was reached (10-15 minutes). Next, 20 μ L of 6.75-fold concentrated stock solutions of an opioid reference standard (in Opti-MEM[®], Opti-MEM[®]/MeOH or Opti-MEM[®]/ACN) or of the obtained powder was added to the cells (concentrations ranging from 100 μ M to 1 pM). To ensure comparability with earlier studies (Vasudevan et al. 2020; Verougstraete et al. 2020; Vandeputte et al. 2021b), hydromorphone was included as a reference agonist for normalization. Etonitazene, fentanyl, and morphine were added to further aid interpretation. Alternatively, 20 μ L of the reconstituted samples was added (cfr. *supra*) rather than opioid stock solutions. In the final step of the assay protocol, luminescence was monitored for a total of 2 hours. Each condition was measured in duplicate in two (urine) or three (reference

standards, powder and serum) independent experiments ($n = 3$), and appropriate (solvent) controls were added on each plate.

Data analysis

After the two-hour read-out, the recorded amount of luminescence (in relative light units, RLU) was plotted over time for each condition. The obtained profiles were corrected for inter-well variability (Pottie et al. 2020). When required, areas under the curve (AUCs) were calculated as previously described (Pottie et al. 2020). After subtraction of the mean AUC of the corresponding control wells, the solvent-corrected AUC values were used to plot concentration-response curves via GraphPad Prism 9 (San Diego, CA, U.S.) using three-parameter nonlinear regression. The data were normalized to the maximum response of hydromorphone (arbitrarily set at 100%) (Vasudevan et al. 2020; Vandeputte et al. 2021b). The standard Grubbs' test was used for outlier testing of the normalized AUC values per compound per concentration, leading to the identification and subsequent exclusion of one value (0.4%). For each compound (reference standards or sourced powder), the normalized data from three independent experiments were then combined to obtain final potency (EC_{50}) and efficacy (E_{max} , relative to hydromorphone) values.

For semi-quantification of the patient samples using the standard addition approach, the corrected AUC values of the patient sample (serum or urine) were compared with that of the fortified sample, allowing calculation of the *N*-piperidinyl etonitazene concentration present in the non-fortified patient sample (i.e., within a limited concentration range, the total luminescence output (AUC value) varies linearly with the total concentration present in the sample, allowing calculation of the unknown concentration). Results are given for one representative experiment (out of $n = 2$ for urine and $n = 3$ for serum).

For determination of fentanyl and hydromorphone MOR activity equivalents, GraphPad Prism 9 (San Diego, CA, U.S.) was used to plot luminescence-time profiles, following correction for inter-well variability, of one representative experiment (out of $n = 2$ independent replicates).

2.10 Pharmacodynamics in rats

Animals and surgery

Male Sprague-Dawley rats (300-400 g) were purchased from Envigo (Frederick, MD, U.S.) and group-housed under controlled conditions (temperature $22 \pm 2^\circ\text{C}$; humidity $45 \pm 5\%$), with ad libitum access to food and water. Lights were on from 7:00 a.m. to 7:00 p.m. The animal

experiments were approved by the NIDA Intramural Research Program (IRP), Animal Care and Use Committee, and all procedures were carried out in accordance with the NIH Guide for the Care and Use of Laboratory Animals. Vivarium facilities were fully accredited by the Association for Assessment and Accreditation of Laboratory Animal Care. Experiments were designed to minimize the number of animals included in the study. Isoflurane was used to anesthetize rats using a drop jar which contained a gauze pad saturated with 2 mL of isoflurane, placed beneath a wire mesh floor. Each anesthetized rat received a subcutaneous (s.c.) temperature transponder (cylindrical shape, 14 x 2 mm, model IPTT-300, Bio Medic Data Systems, Seaford, DE, U.S.) that emits radio frequency signals to a compatible hand-held reader system (DAS-7006/7r, Bio Medic Data Systems). This allowed for the non-invasive measurement of body temperature (Bergh et al. 2021). The transponders were implanted on the back using a pre-packaged sterile guide needle. After the procedure, rats were single-housed and given at least 1 week to recover.

Experimental procedures

On the day of an experiment, rats were brought into the laboratory in their home cages and allowed 1 h to acclimate. A total of six rats per dose group ($n = 6$) received s.c. injections of vehicle (1 mL/kg, 10% DMSO in saline) or *N*-piperidinyl etonitazene (0.003-0.100 mg/kg) on the lower back between the hips. Separate groups of rats ($n = 6$ per dose group) received morphine (1.0 - 30 mg/kg, s.c.), fentanyl (0.003 - 0.10 mg/kg, s.c.), or saline vehicle (1 mL/kg, s.c.), as reported elsewhere (Vandeputte & Krotulski *et al.*, manuscript submitted). After injections, the rats were returned to their home cages. Doses were randomly assigned, and each rat was tested twice in separate experimental sessions at least three days apart to ensure washout. Pharmacodynamic endpoints, including catalepsy score, body temperature, and hot plate latency, were determined prior to injection and at 15, 30, 60, 120, and 240 min post-injection (Bergh et al. 2021). At each time point, behavior was observed for 1 min by an experienced rater. Catalepsy was scored based on three overt symptoms (immobility, flattened body posture, and splayed limbs), that were scored as either '1=absent' or '2=present'. Catalepsy scores at each time point were summed, yielding a minimum score of 3 and a maximum score of 6. Next, body temperature was measured using a handheld reader sensitive to signals emitted by the surgically implanted transponder (cfr. *supra*). Hypothermia was selected as a representative adverse effect of opioid treatment, since body temperature is a convenient physiological measure that has been shown to decrease in parallel with opioid-

induced bradycardia and respiratory depression (Wong et al. 2017). Finally, rats were placed on a hot plate analgesia meter (IITC Life Sciences, Woodland Hills, CA, U.S.) set at 52°C. The animals remained on the hot plate until hind paw licking was observed in response to the heat stimulus, upon which they were returned to their home cages. The total time spent on the hot plate was recorded by means of a timer triggered by a foot pedal. A 45 sec cut-off was employed to prevent tissue damage.

Data analysis

Pharmacodynamic findings were analyzed using GraphPad Prism. Raw data for hot plate latency and catalepsy score over time were normalized to the percent maximum possible effect (%MPE) (**Equation 1**).

$$\frac{\text{experimental measure} - \text{baseline measure}}{\text{maximum possible response} - \text{baseline measure}} \times 100 \quad \text{Eq. 1}$$

The MPEs for hot plate latency and catalepsy score were 45 sec and 6, respectively. Raw time-course data for body temperature were normalized to change from baseline for each rat (Δ temperature in °C). To determine effects of drug doses at each time point, normalized time-course data were analyzed by two-factor (dose x time) ANOVA followed by Tukey's post hoc test. Mean hot plate latency and catalepsy score over the first 60 min were used to obtain dose-response relationships. Potency (ED_{50}) values were determined via non-linear regression (response stimulation, normalized response).

3. Results

3.1 Analysis of *N*-piperidinyl etonitazene

LC-HRMS, GC-MS, UHPLC-DAD and FT-IR

LC-HRMS analysis of the powder in full scan mode revealed a single peak with a retention time of 5.42 minutes and an exact m/z value of 409.2227, resulting in a mass deviation of -1.71 ppm compared to the single-protonated exact mass of 409.2234 in the HighResNPS library (Mardal et al. 2019). The obtained fragment ion spectrum of *N*-piperidinyl etonitazene is shown in **Figure 4A**: the four main product ions had an m/z value of 84.0812 (corresponding to the piperidinyl ring fragment; $C_5H_{10}N^+$), 107.0493 (3-hydroxybenzyl, a common product ion of 2-benzylbenzimidazole opioids (Vandeputte et al. 2021b); $C_7H_7O^+$), 112.1122 ($C_7H_{14}N^+$) and 135.0805 ($C_9H_{11}O^+$). Both the retention time (difference 0.06 min) and the fragment ion spectrum matched with that of the Cayman reference standard (data not shown).

N-piperidinyl etonitazene eluted after 12.68 minutes in the GC-MS analysis. The obtained GC-MS spectrum is shown in **Figure 4B**. HPLC-DAD analysis revealed a single peak with a retention time of 1.38 minutes showing absorption maxima at 241 and 309 nm (**Figure 4C**). FT-IR analysis of the powder using attenuated total reflectance showed main absorbance peaks at 1510, 1336, 1316, 1233 and 738 cm^{-1} (**Figure 4D**). The IR spectrum did not match any entry from an in-house library.

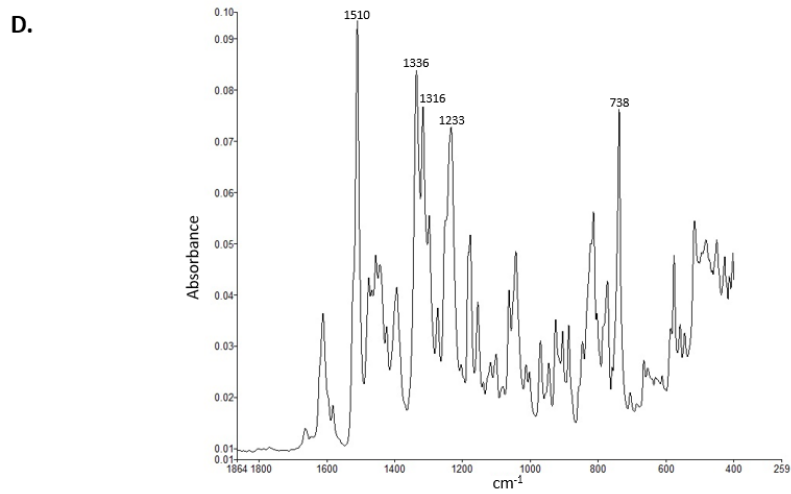
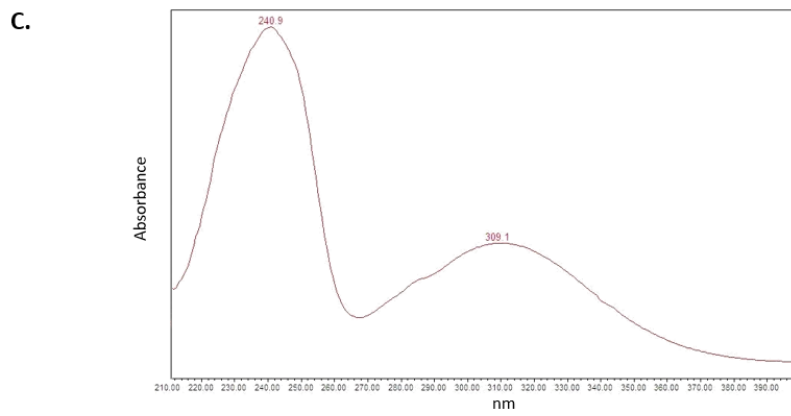
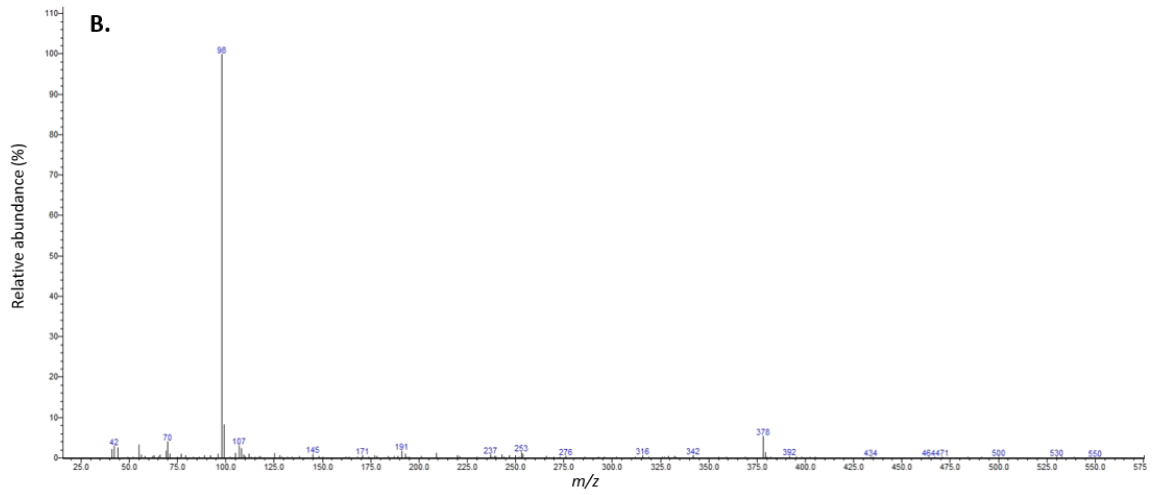
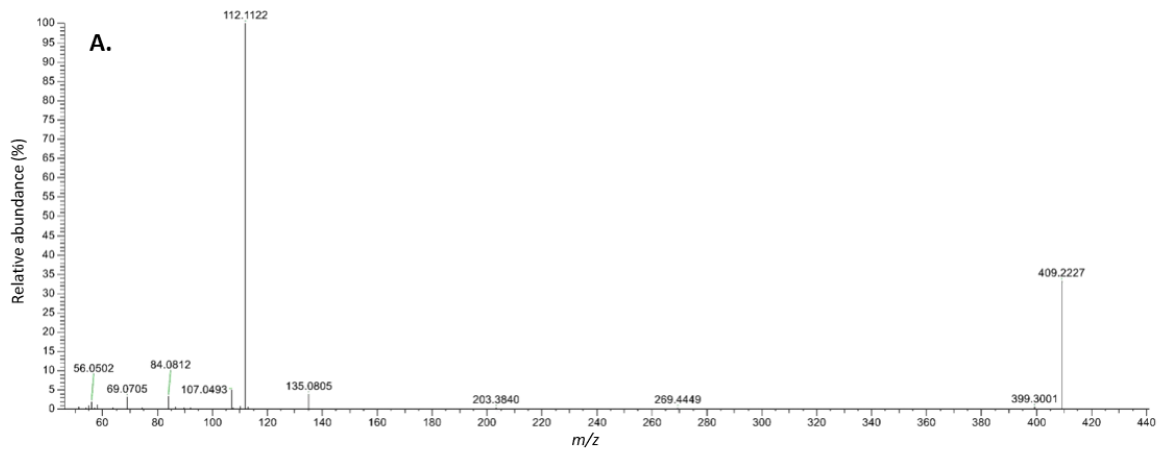


Figure 4. **A.** HRMS fragment ion spectrum; **B.** GC-MS electron ion impact spectrum; **C.** HPLC-DAD spectrum; **D.** FT-IR spectrum of the *N*-piperidinyl etonitazene powder.

In vitro pharmacological characterization

Radioligand binding experiments were performed to evaluate the binding affinity of *N*-piperidinyl etonitazene at MOR, the main opioid receptor responsible for most clinically and toxicologically relevant opioid effects (**Figure 5** and **Table 1**). Our findings indicate that *N*-piperidinyl etonitazene has a high MOR affinity, albeit somewhat lower than the MOR affinities of fentanyl and morphine (2.3- and 3.6-fold, respectively).

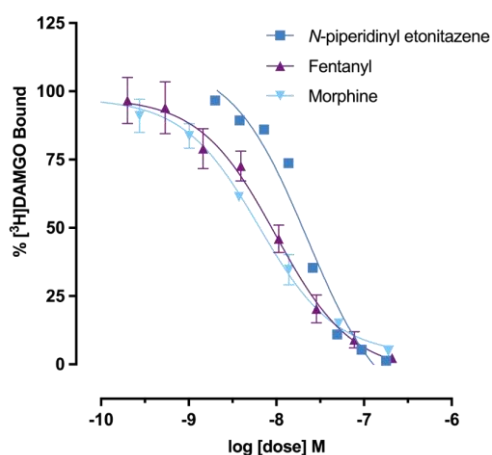


Figure 5. MOR binding curves for *N*-piperidinyl etonitazene, fentanyl, and morphine in rat brain tissue. Data are plotted as mean \pm standard deviation (SD) for % ^3H]DAMGO bound.

Table 1. MOR affinities of *N*-piperidinyl etonitazene, fentanyl and morphine. K_i values (nM) are given as mean \pm SD for $n = 3$ experiments, each performed in triplicate.

K_i values (nM)	MOR [^3H]DAMGO
<i>N</i> -piperidinyl etonitazene	14.3 \pm 2.5
Fentanyl	6.17 \pm 0.82
Morphine	3.99 \pm 0.40

In addition to the high MOR affinity of *N*-piperidinyl etonitazene, evaluation of the intrinsic MOR activation potential revealed high *in vitro* potency and relative efficacy (**Figure 6** and **Table 2**). *N*-piperidinyl etonitazene was 53 and 6.7 times more potent than morphine and

fentanyl, respectively, and also exceeded the efficacy of both opioids. While equally efficacious with etonitazene, *N*-piperidinyl etonitazene was about 6.7 times less potent than the *N,N*-diethyl analogue. The obtained concentration-response curves of the sourced *N*-piperidinyl etonitazene powder overlapped with that of the reference standard, indicating high purity of the powder.

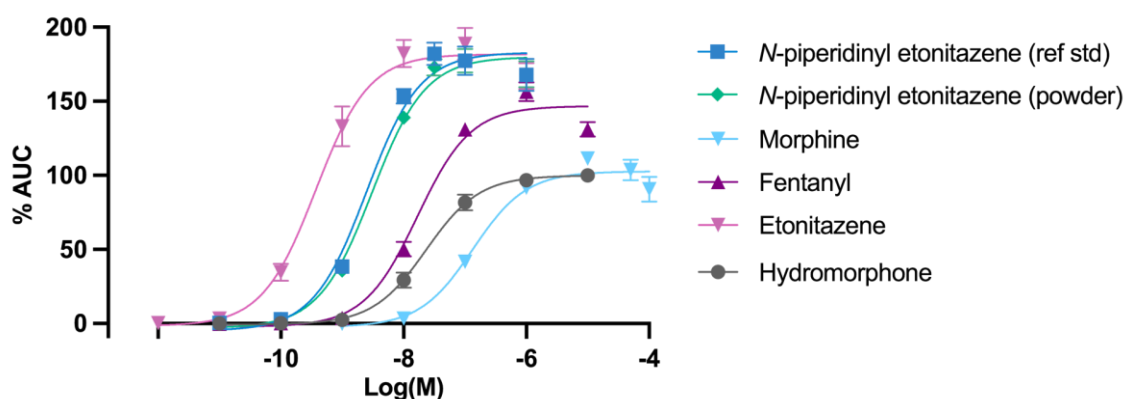


Figure 6. μ -Opioid receptor activation profiles ($n = 3$) for *N*-piperidinyl etonitazene (reference standard and sourced powder) and various comparator opioids. Data are given as mean receptor activation \pm standard error of the mean (SEM), and are normalized to the maximum response of hydromorphone.

Table 2. Overview of potency (EC_{50}) and efficacy (E_{max} , relative to hydromorphone) values as obtained in the MOR activation assay. 95% confidence intervals are indicated between brackets.

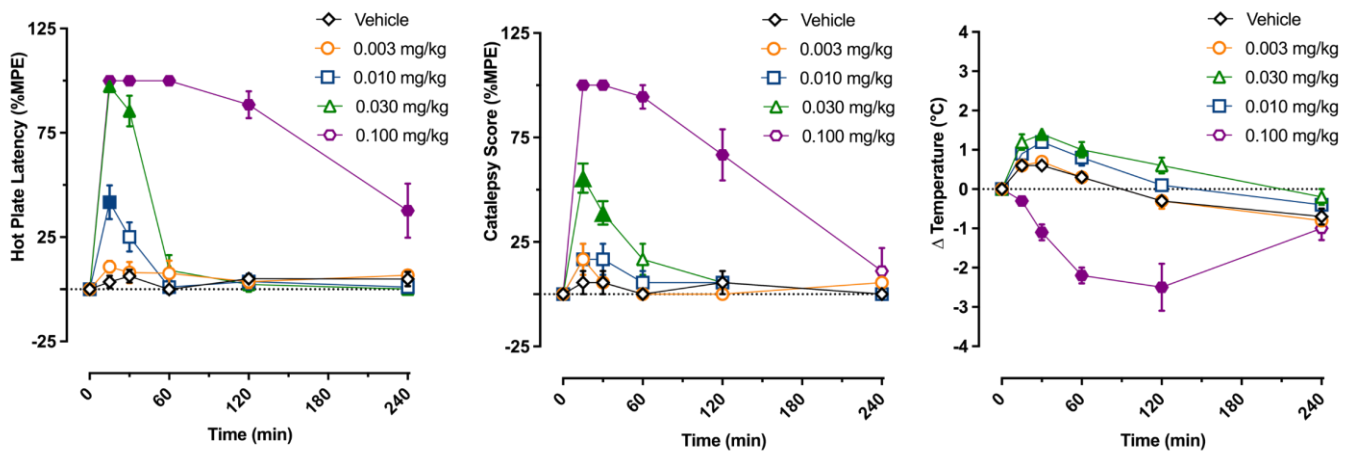
	EC_{50} (nM)	E_{max} (% of hydromorphone)
<i>N</i> -piperidinyl etonitazene reference standard	2.49 (1.67-3.74)	183 (173-194)
<i>N</i> -piperidinyl etonitazene sourced powder	3.06 (2.19-4.26)	180 (172-189)
Morphine	134 (80.8-228)	103 (96.2-109)
Fentanyl	16.8 (11.7-24.4)	147 (139-155)
Etonitazene	0.370 (0.232-0.585)	182 (171-193)
<i>Hydromorphone</i>	23.2 (16.8-32.4)	99.9 (95.1-105)

In vivo pharmacological characterization

Figure 7A displays the pharmacodynamic effects induced by s.c. administration of *N*-piperidinyl etonitazene in rats. Two-way ANOVA (dose x time) revealed that *N*-piperidinyl etonitazene induced significant effects on hot plate latency ($F[4,145] = 213.7$, $p < 0.0001$),

catalepsy score ($F[4,144] = 131.8, p < 0.0001$), and body temperature ($F[4,150] = 93.90, p < 0.0001$). Rats treated with *N*-piperidinyl etonitazene showed dose-dependent increases in hot plate latency, indicating antinociceptive effects of the drug at different doses. Post-hoc tests revealed that, at the lowest dose injected (0.003 mg/kg), no statistically significant change in hot plate latency was found compared to the control group. Significant differences in latency were seen at 15 minutes for rats receiving 0.010 mg/kg *N*-piperidinyl etonitazene, and at 15 and 30 minutes for rats receiving 0.030 mg/kg *N*-piperidinyl etonitazene. The most sustained increases in hot plate latency were seen at the highest dose of 0.100 mg/kg *N*-piperidinyl etonitazene, starting at 15 min post-injection. The maximum cut-off latency of 45 s was reached in the groups receiving the two highest doses (0.030 mg/kg and 0.100 mg/kg). Following nonlinear regression analysis of the mean hot plate responses over 60 min, the ED_{50} value for *N*-piperidinyl etonitazene was 0.0205 mg/kg (**Figure 7B**). Clear signs of dose-dependent catalepsy were observed at the two highest doses after 15 minutes. The most sustained cataleptic effects were again seen in rats receiving the highest dose of *N*-piperidinyl etonitazene (0.100 mg/kg), with a significant catalepsy score until 120 min post-injection. With an ED_{50} value of 0.0354 mg/kg, the potency for *N*-piperidinyl etonitazene-induced catalepsy was slightly lower than that found for antinociception. The 0.030 mg/kg dose of *N*-piperidinyl etonitazene induced small but significant increases in body temperature at 30 and 60 min post-injection. However, a pronounced and sustained drop in body temperature was observed after injection of the highest dose (0.100 mg/kg). In line with the profile of effects produced by *N*-piperidinyl etonitazene, both fentanyl and morphine produced significant time-dependent effects on hot plate latency, catalepsy scores, and body temperature (**Supplementary Figures S1A-B**). The ED_{50} values for fentanyl- and morphine-induced antinociception were 0.0209 and 3.940 mg/kg, respectively (**Figure 7B**) (Vandeputte & Krotulski *et al.*, in press). Thus, our data demonstrate that the antinociceptive potency of *N*-piperidinyl etonitazene is nearly equivalent to that of fentanyl and 192-fold greater than that of morphine in rats.

A.



B.

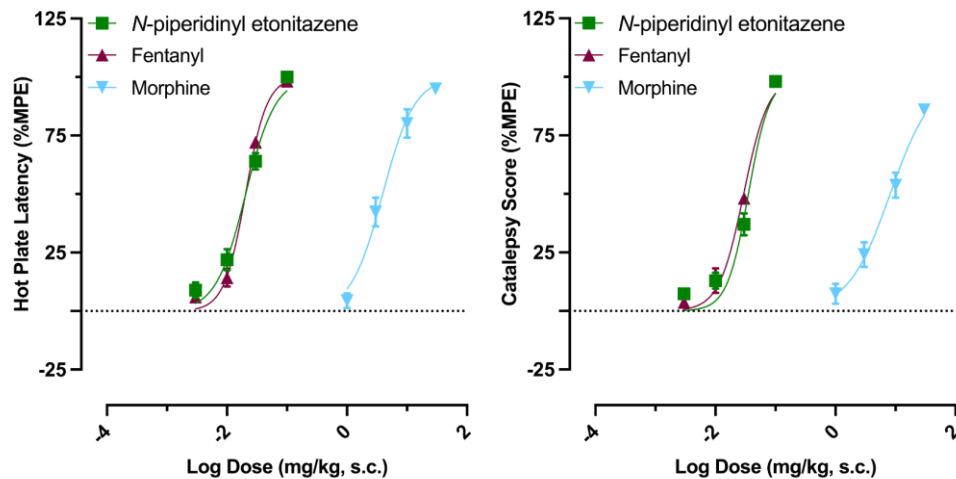


Figure 7. A. Time course of pharmacodynamic effects induced by subcutaneous 10% DMSO (vehicle, 1 mL/kg) or *N*-piperidinyl etonitazene (0.003, 0.010, 0.030, 0.100 mg/kg) in male rats. Hot plate latency, catalepsy score, and body temperature are shown as mean \pm SEM ($n = 6$ rats/dose group). Hot plate latency and catalepsy scores are presented as a percent of maximum possible effect (%MPE), while temperature data are expressed as change from baseline (Δ temperature in $^{\circ}$ C). Filled symbols indicate significant differences as compared to the vehicle-treated group at a given time point ($p < 0.05$, Tukey's). **B.** Dose-response curves obtained from nonlinear regression analysis (response stimulation normalized slope) of the mean hot plate responses and catalepsy scores (expressed as % MPE) over the first 60 min for *N*-piperidinyl etonitazene, fentanyl, and morphine ($n = 6$ rats per dose group). Error bars represent SEM.

3.2 Analysis of patient samples via LC-HRMS and the MOR bioassay

LC-HRMS

The *N*-piperidinyl etonitazene concentration was 1.21 ng/mL in serum and 0.51 ng/mL in urine. Concentrations obtained via standard addition were in line with those calculated via the calibration curves. Moreover, the benzodiazepines diazepam (+ metabolites nordiazepam, temazepam, oxazepam), lorazepam, clonazepam (+ metabolite 7-aminoclonazepam) and etizolam (+ metabolite alpha-hydroxyetizolam), the latter belonging to the group of NPS benzodiazepines, were found both in the serum and urine sample. Pregabalin was also detected in the samples. No other opioids were found. Via molecular networking using the GNPS software, five possible metabolites were identified in the urine sample of the patient (**Table 3** and **Figure 8**). De-alkylation, resulting in the *O*-desalkyl metabolite M1, was identified as the primary metabolism route. Reduction of the nitro group resulted in M2, and the products of hydroxylation of the piperidinyl ring (M3) with subsequent oxidation (M4) were also detected. The presence of M5, an *O*-desalkyl metabolite of *N*-pyrrolidino etonitazene, was also picked up. None of the five tentative urinary metabolites were detected in the serum sample.

Table 3. Tentatively identified metabolites of *N*-piperidinyl etonitazene in urine.

ID	Biotransformation	Formula	<i>m/z</i> (H+) theoretical	<i>m/z</i> (H+) measured	Mass error (ppm)	Retention time (min)	Base peak of MS2 spectrum
P0	Parent drug	C ₂₃ H ₂₈ N ₄ O ₃	409.2233	409.2236	0.5	5.48	112.1124
M1	<i>O</i> -dealkylation	C ₂₁ H ₂₄ N ₄ O ₃	381.1929	381.1929	0	4.48	112.1124
M2	<i>O</i> -dealkylation + nitro reduction	C ₂₁ H ₂₆ N ₄ O	351.2184	351.2176	-2.3	1.89	112.1124
M3	<i>O</i> -dealkylation + hydroxylation of piperidinyl ring	C ₂₁ H ₂₄ N ₄ O ₄	397.1870	397.1870	0	3.99	128.1072
M4	<i>O</i> -dealkylation + ketone on the piperidinyl ring	C ₂₁ H ₂₂ N ₄ O ₄	395.1706	395.1715	2.3	5.77	126.0916
M5	<i>O</i> -dealkylation + contraction of piperidinyl ring	C ₂₀ H ₂₂ N ₄ O ₃	367.1765	367.1765	0	4.32	98.0969

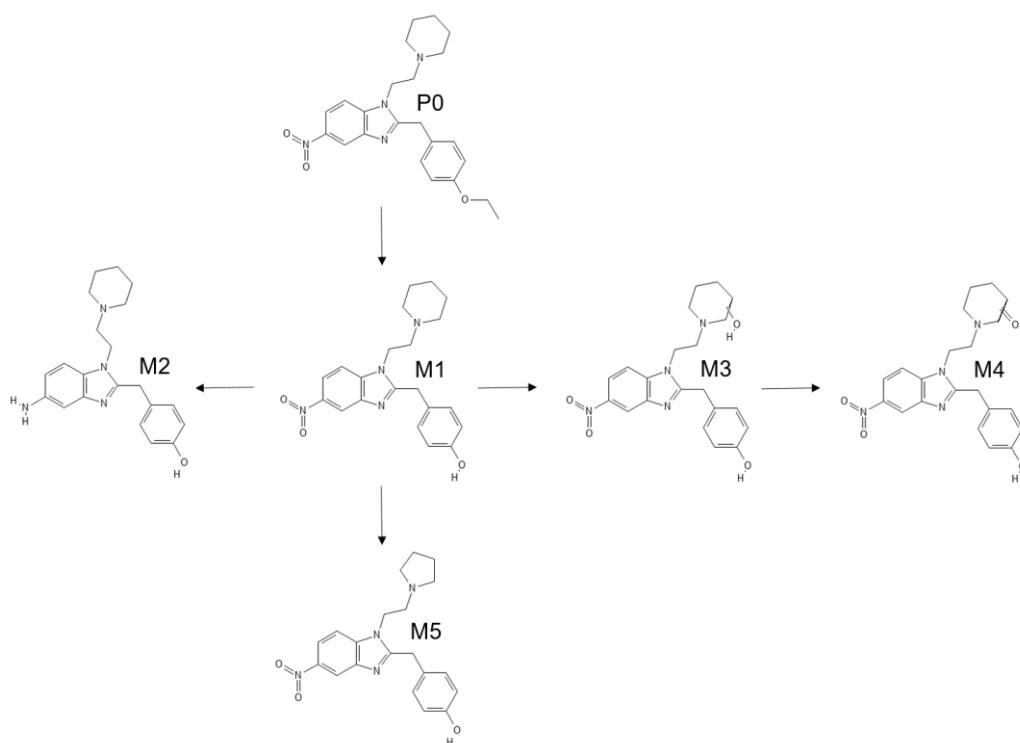
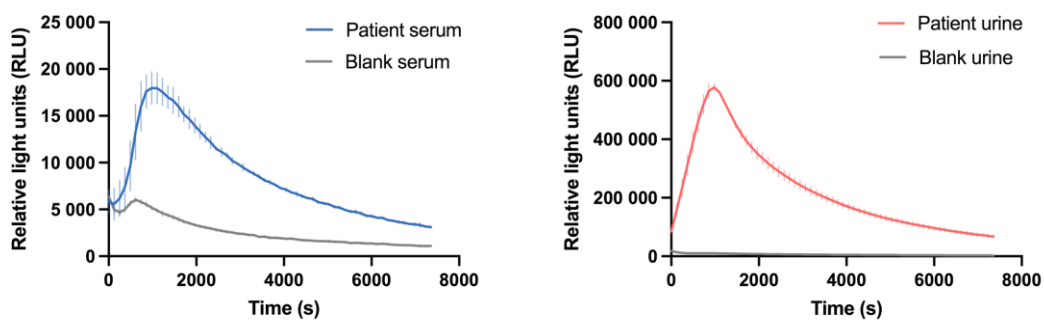


Figure 8. Proposed metabolism scheme for *N*-piperidinyl etonitazene (P0). See text for details.

Bioassay

The presence of opioid activity in both patient serum and urine was confirmed by means of the MOR activation bioassay, as a signal clearly distinct from blank was observed (**Figure 9**).

A.



B.

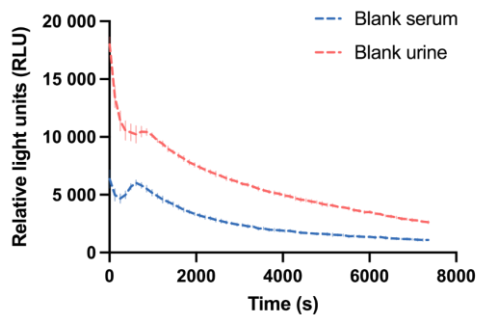


Figure 9. μ -Opioid receptor (MOR) activation as exerted by authentic serum and urine samples. **A.** Patient serum (left panel) and urine (right panel). **B.** Zoom-in of the profiles obtained for blank serum and blank urine. The difference in baseline signal indicates the presence of a matrix effect. Results are shown as mean receptor activation \pm standard deviation of one representative experiment, in which each sample was run in duplicate. Note the difference in scales of the y-axes.

Secondly, apart from a qualitative assessment of the presence of opioid activity, the bioassay also allows semi-quantification (Cannaert et al. 2020). Using the bioassay, the employed standard addition approach revealed concentrations for *N*-piperidinyl etonitazene in the low ng/mL range in serum (median ($n=3$) = 1.88 ng/mL), which is in line with the detected analytical concentration (1.21 ng/mL). In urine, the obtained signal consistently indicated a concentration of around 2 ng/mL, whereas the analytical concentration was only 0.51 ng/mL, potentially indicating the presence of active metabolites in urine.

Finally, the use of the bioassay also allows insight into the extent of opioid activity exerted by *N*-piperidinyl etonitazene in the patient (Verougstraete et al. 2020). Our data show that the MOR activity exerted by 1 ng/mL *N*-piperidinyl etonitazene (as approximately present in the patient's serum) corresponds to that of a concentration between 2.5 and 10 ng/mL fentanyl or 10 and 25 ng/mL hydromorphone in serum (**Figure 10**).

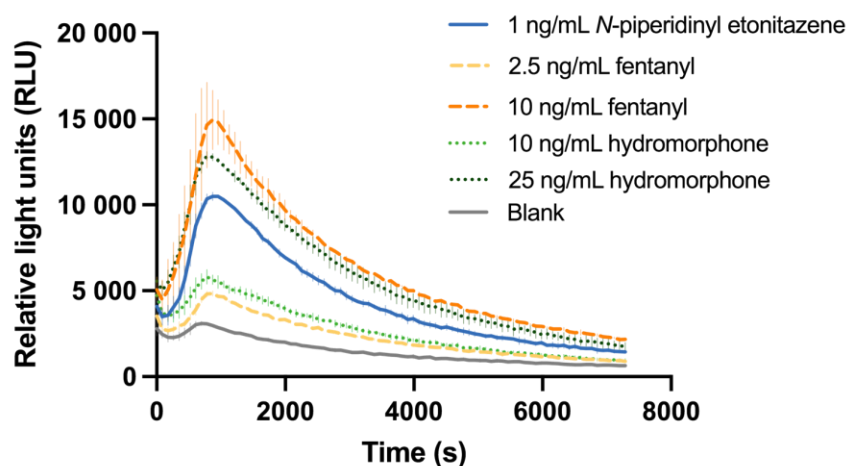


Figure 10. Activity equivalents plot indicating that the activity exerted by a 1 ng/mL concentration of *N*-piperidinyl etonitazene (as approximately present in the patient's serum sample) is equivalent to that exerted by 2.5-10 ng/mL fentanyl or 10-25 ng/mL hydromorphone. Results are shown as mean

receptor activation \pm standard deviation of one representative experiment, in which each sample was run in duplicate.

4. Discussion

N-piperidinyl etonitazene ('etonitazepipne') is one of the most recent synthetic opioids to emerge on recreational drug markets in the U.S. and Europe. With its characteristic 2-benzylbenzimidazole core structure, the drug represents one of the latest additions to the increasingly widespread group of 'nitazene' opioids. Interestingly, a related cyclic analogue of etonitazene (*N*-pyrrolidino etonitazene or 'etonitazepyne' (Vandeputte & Krotulski *et al.*, in press)) also recently appeared in recreational drug markets. In this work, we describe the first identification, chemical analysis and pharmacological characterization of *N*-piperidinyl etonitazene. An online-sourced powder was obtained from a patient pursuing help for detoxification. Using a broad spectrum of analytical techniques (LC-HRMS, GC-MS, LC-DAD, and FT-IR), the powder was unambiguously identified as *N*-piperidinyl etonitazene. Although no exhaustive attempts to unequivocally prove the purity of the powder were undertaken, the obtained spectra were indicative of a highly pure powder, as no evidence of impurities (e.g., additional peaks suggesting the presence of impurities) could be detected. This was further supported by the results obtained in the *in vitro* MOR activation assay, which showed an overlap between the concentration-response curves of the powder and a reference standard.

Radioligand binding experiments showed that *N*-piperidinyl etonitazene has a high affinity for MOR ($K_i = 14.3 \pm 2.5$ nM), the primary opioid receptor implicated in most therapeutic (e.g., analgesic) and adverse (e.g., respiratory depression) opioid effects (Williams *et al.* 2013). *N*-piperidinyl etonitazene showed a lower binding affinity than morphine (3.99 ± 0.40 nM) and fentanyl (6.17 ± 0.82 nM). However, confirming earlier observations (Volpe *et al.* 2011; Baumann *et al.* 2018) that binding affinity may not predict the functional activity of a drug, we found that *N*-piperidinyl etonitazene was over 50 times more potent and 80% more efficacious than morphine in activating human MOR. The drug further exceeded the *in vitro* potency of fentanyl by 6.7 times, and reached a 36% higher relative efficacy than fentanyl. *N*-piperidinyl etonitazene was equally efficacious and about 6.7 times less potent than its *N,N*-diethyl analogue etonitazene, the most potent 2-benzylbenzimidazole opioid identified to date (Vandeputte *et al.* 2021b). Interestingly, the *in vivo* effect profile of *N*-piperidinyl etonitazene in male rats showed a slightly different picture. While *N*-piperidinyl etonitazene was > 190

times more potent than morphine in its ability to induce antinociception (in line with early studies conducted in mice (Hunger et al. 1960b)), the dose-response curves of fentanyl and *N*-piperidinyl etonitazene overlapped, indicating similar *in vivo* potency to induce antinociception in rats. Hence, relative to fentanyl, the potency of *N*-piperidinyl etonitazene appears to be somewhat overestimated using the employed *in vitro* functional assay. While further research is needed, the difference between *in vitro* and *in vivo* potency trends could be explained by several factors, such as a limited half-life of *N*-piperidinyl etonitazene in the rat. Given that a highly similar cyclic analogue of etonitazene, *N*-pyrrolidino etonitazene (Vandeputte & Krotulski, in press), did exceed the *in vitro* and *in vivo* potency of fentanyl (as determined using the same assays employed in the current study), it is unlikely that a decreased blood-brain barrier permeability of the more lipophilic *N*-piperidinyl etonitazene can explain these observations. In addition, it should be noted that the employed *in vitro* functional assay monitors recruitment of β arr2 to human MOR, whereas eventual *in vivo* effects are the result of complex intracellular signaling, involving a multitude of pathways, following rat MOR activation. *N*-piperidinyl etonitazene further showed characteristic opioid-mediated behavior in rats: its catalepsy-inducing potency was slightly lower than that observed for hot plate latency (Pöyhiä and Kalso 1992; Taracha et al. 2009; Truver et al. 2020; Bergh et al. 2021), and a typical biphasic effect on body temperature – with hypothermia at the highest dose injected – was observed (Geller et al. 1983; Adler et al. 1988; Rawls and Benamar 2011). Similar trends in opioid-mediated effects were seen for morphine and fentanyl, when administered at appropriate doses (**Supplementary Information S1**). For *N*-piperidinyl etonitazene and fentanyl, the body temperature reached its nadir at the highest injected dose of 0.1 mg/kg. Hence, in line with the results of the hot plate latency and catalepsy assays, both drugs are similar in their ability to produce hypothermia in the rat. Compared to morphine, *N*-piperidinyl etonitazene was about 300 times more potent in producing hypothermia. Although further research is warranted to confirm this hypothesis, the difference in dose required to induce significant antinociception (0.010 mg/kg) vs hypothermia (0.100 mg/kg) in opioid-naïve rats corroborates that higher doses of *N*-piperidinyl etonitazene are likely needed to produce adverse opioid effects. Importantly, at this point it is not clear how - and if - these findings can be translated to humans.

Prior to quantitative analysis, the presence of opioid activity in two authentic samples (serum and urine) was detected by means of an activity-based screening assay (**Figure 9**) (Cannaert et al. 2018). This underscores the potential of this bioassay as a first-line screening tool for the universal detection of opioid NPS in biological samples (Cannaert et al. 2018): given the novelty of *N*-piperidinyl etonitazene on the recreational drug market, conventional screening techniques (e.g., immunoassays) and targeted analysis using libraries of known compounds may fail to detect the presence of a novel unknown opioid in biological samples. Activity-based screening, on the other hand, has the important benefit of being an untargeted approach, not requiring prior knowledge of a compound. Quantitative analysis of *N*-piperidinyl etonitazene in authentic biological samples via LC-HRMS revealed concentrations of 1.21 ng/mL in serum and 0.51 ng/mL in urine. These concentrations are comparable with reported nitazene analogue concentrations from forensic casework samples in the sub and low ng/mL range (Walton et al. 2021) (Vandeputte & Krotulski *et al.*, in press). The presence of low ng/mL *N*-piperidinyl etonitazene concentrations in biological samples highlights the need for highly sensitive analytical methods for drug detection and quantification. While no other opioids were detected in the analyzed samples, various benzodiazepines were identified alongside *N*-piperidinyl etonitazene. The combination of (NPS) benzodiazepines with nitazene opioids has previously been reported in cases involving isotonitazene, metonitazene and *N*-pyrrolidino etonitazene (Krotulski et al. 2020, 2021b) (Vandeputte & Krotulski *et al.*, in press).

Further analysis of the biological samples resulted in the tentative identification of five urinary *N*-piperidinyl etonitazene metabolites (**Figure 8 + Table 3**). In line with previous findings for other 2-benzylbenzimidazole opioids like isotonitazene (Krotulski et al. 2020), metonitazene (Krotulski et al. 2021b), and etodesnitazene (Grigoryev et al. 2022), *N*-piperidinyl etonitazene was found to undergo *O*-de-alkylation as the primary metabolism route, resulting in the *O*-desalkyl metabolite M1. As also described for isotonitazene (Krotulski et al. 2020) and metonitazene (Krotulski et al. 2021b), the nitro group was reduced to form M2. Also, hydroxylation of the piperidinyl ring was found to occur (M3), with subsequent oxidation to form a ketone on the piperidinyl ring (M4). The presence of M5 (the *O*-desalkyl metabolite of *N*-pyrrolidino etonitazene (Vandeputte & Krotulski *et al.*, in press)) could be the result of an unusual contraction of the piperidinyl ring catalyzed by CYP3A4 (Ortiz de Montellano and Nelson 2011). However, this hypothesis should be confirmed via comparative analysis of urine

samples of an *N*-pyrrolidino etonitazene user, or via a reference standard of *O*-desalkyl *N*-pyrrolidino etonitazene. None of the five urinary metabolites were found in the corresponding serum sample. Peak areas for the proposed metabolites were slightly higher after glucuronide hydrolysis as compared to unhydrolyzed urine. Moreover, M2 was only found after hydrolysis, suggesting that at least some of these metabolites undergo an additional glucuronide conjugation. However, the role of glucuronide conjugation could not be unequivocally confirmed as no glucuronide conjugates were found in the original urine sample. In comparison, no phase II metabolites (glucuronides, sulphates or glutathionates) were found for etodesnitazene (Grigoryev et al. 2022), and for isotonitazene the impact of hydrolysis was reported to be minimal as well (Krotulski et al. 2020). It should also be noted that our *N*-piperidinyl etonitazene metabolite discovery experiment was only performed on one patient sample, with only a limited amount of urine being available.

The presence of potentially active metabolites in urine may explain why the bioassay indicated a higher concentration of *N*-piperidinyl etonitazene in urine than in serum, as opposed to the analytical findings. In other words, the apparent discrepancy between the analytical urinary concentration (0.51 ng/mL *N*-piperidinyl etonitazene) and the 4 times higher estimated urinary concentration obtained with the bioassay might be explained by the presence of potentially active metabolites in urine, contributing to the overall opioid-like signal obtained in the bioassay. Hence, this result suggests that at least some of the urinary metabolites retain opioid activity, as has been previously shown for various nitazene metabolites (Vandeputte et al. 2021b). However, further research is warranted to confirm this hypothesis. The obtained result in urine also illustrates an inherent strength of the use of activity-based assays for screening purposes: as the obtained signal will be the result of receptor activation by all MOR agonists present in the sample, this increases the sensitivity of the methodology (i.e., while the activity of individual compounds - parent and metabolites - may not be detectable, the combined activity will result in a signal sufficiently different from blank).

In a related context, another highly useful application of the bioassay lies in its ability to determine 'activity-equivalents' (Verougstraete et al. 2020). This is particularly relevant, as it is very hard to interpret what a serum concentration of 1.21 ng/mL *N*-piperidinyl etonitazene actually means. Using the bioassay, we show that the level of opioid activity (a combination

of the potency and efficacy of a drug) present in the patient's serum (approximately 1 ng/mL *N*-piperidinyl etonitazene) is equivalent to the *in vitro* opioid activity exerted by 2.5-10 ng/mL fentanyl or 10-25 ng/mL hydromorphone in serum (**Figure 10**). With the caveat that *in vitro* findings may not be directly translatable to the *in vivo* situation (cfr. *supra*), this information allows a better interpretation of the reported concentration in this case: as the opioid activity present in the patient's serum is equivalent to that of a fentanyl serum concentration in the low ng/mL range (which, in opioid-naïve individuals, may already lead to a fatal outcome), it can be deduced that the patient, who presented to his general practitioner with a normal level of consciousness, had acquired a high opioid tolerance. This hypothesis is in agreement with the case history.

5. Conclusion

This study presents the first identification, chemical analysis, and pharmacological characterization of *N*-piperidinyl etonitazene (etonitazepipne), one of the latest additions to the rapidly expanding class of 2-benzylbenzimidazole ‘nitazene’ opioids on the recreational NPS market. *N*-piperidinyl etonitazene was identified for the first time in an online-sourced powder and in the serum and urine of a patient. Various metabolites of the drug were tentatively identified in urine. Furthermore, our *in vitro* and *in vivo* findings demonstrate that *N*-piperidinyl etonitazene is a potent MOR agonist. Taken together, our data indicate that the misuse of *N*-piperidinyl etonitazene (etonitazepipne) is of great concern to public health.

Funding

This work was supported by the Research Foundation-Flanders (FWO) [1S81522N to M.V., 1703320N to N.V, and G069419N to C.S.] and the Ghent University Special Research Fund (BOF) [01J15517 to C.S.]. Dr. Baumann's research is generously supported by the Intramural Research Program (IRP) of the National Institute on Drug Abuse (NIDA), National Institutes of Health, U.S.

Acknowledgements

The patient is gratefully acknowledged for the cooperation. We kindly thank Dr. Donna Iula (Cayman Chemical) for gifting of the *N*-piperidinyl etonitazene reference standard.

(Supplementary Figures are included after the references)

Conflict of interest statement

The authors declare that they have no conflict of interest.

References

- Adler MW, Geller EB, Rosow CE, Cochin J (1988) The Opioid System and Temperature Regulation. *Annu Rev Pharmacol Toxicol* 28:429–449. <https://doi.org/10.1146/annurev.pa.28.040188.002241>
- Baumann MH, Kopajtic TA, Madras BK (2018) Pharmacological Research as a Key Component in Mitigating the Opioid Overdose Crisis. *Trends in Pharmacological Sciences* 39:995–998. <https://doi.org/10.1016/j.tips.2018.09.006>
- Bergh MS-S, Bogen IL, Garibay N, Baumann MH (2021) Pharmacokinetics and pharmacodynamics of cyclopropylfentanyl in male rats. *Psychopharmacology* 238:3629–3641. <https://doi.org/10.1007/s00213-021-05981-x>
- Brandenberger H (1974) Die Rolle des Massenspektrometers im toxikologisch-chemischen Laboratorium. *Deutsche Lebensmittel-Rundschau* 70(1):31–39
- Bromig G (1958) Über neue starkwirkende Analgetika und ihre klinische Erprobung. *Klinische Wochenschrift* 36:960–963. <https://doi.org/10.1007/BF01486702>
- Cannaert A, Deventer M, Fogarty M, et al (2019) Hide and Seek: Overcoming the Masking Effect of Opioid Antagonists in Activity-Based Screening Tests. *Clinical Chemistry* 65:1604–1605. <https://doi.org/10.1373/clinchem.2019.309443>
- Cannaert A, Ramírez Fernández M del M, Theunissen EL, et al (2020) Semiquantitative Activity-Based Detection of JWH-018, a Synthetic Cannabinoid Receptor Agonist, in Oral Fluid after Vaping. *Anal Chem* 92:6065–6071. <https://doi.org/10.1021/acs.analchem.0c00484>
- Cannaert A, Vasudevan L, Friscia M, et al (2018) Activity-based concept to screen biological matrices for opiates and (synthetic) opioids. *Clinical Chemistry* 64:1221–1229. <https://doi.org/10.1373/clinchem.2018.289496>
- Ciccarone D (2019) The triple wave epidemic: Supply and demand drivers of the US opioid overdose crisis. *International Journal of Drug Policy* 71:183–188. <https://doi.org/10.1016/j.drugpo.2019.01.010>
- EMCDDA (2021) European drug report 2021: trends and developments. Publications Office of the European Union, Luxembourg
- EMCDDA (2020) Report on the risk assessment of N,N-diethyl-2-[[4-(1-methylethoxy)phenyl]methyl]-5-nitro-1Hbenzimidazole-1-ethanamine (isotonitazene) in accordance with Article 5c of Regulation (EC) No 1920/2006 (as amended). Publications Office, Luxembourg
- Geller EB, Hawk C, Keinath SH, et al (1983) Subclasses of opioids based on body temperature change in rats: Acute subcutaneous administration. *Journal of Pharmacology and Experimental Therapeutics* 225:391–398

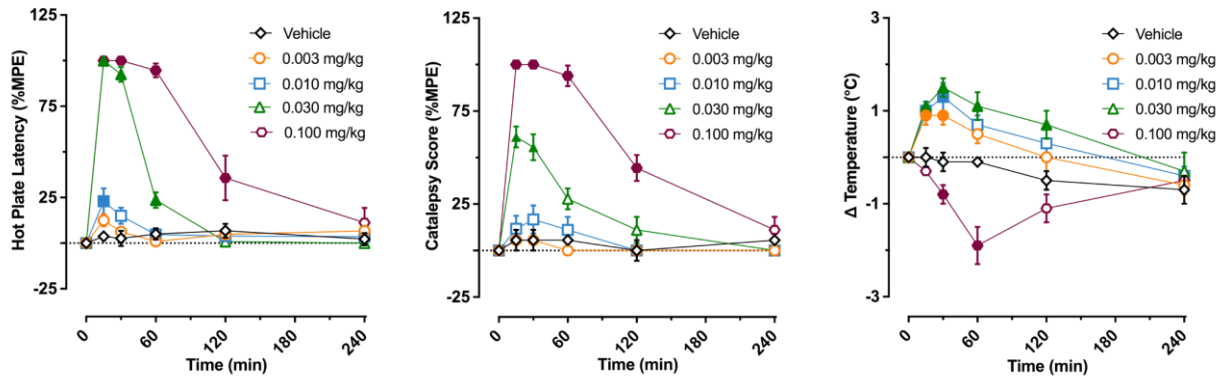
- Grigoryev A, Kavanagh P, Dowling G, Rodin I (2022) Tentative Identification of Etazene (etodesnitazene) Metabolites in Rat Serum and Urine by Gas Chromatography-Mass Spectrometry and Accurate Mass Liquid Chromatography-Mass Spectrometry. *Journal of Analytical Toxicology* bkac001. <https://doi.org/10.1093/jat/bkac001>
- Gross F, Turrian H (1957) Über Benzimidazolderivate mit starker analgetischer Wirkung. *Experientia* 13:401–403. <https://doi.org/10.1007/BF02161117>
- Hunger A, Kebrle J, Rossi A, Hoffmann K (1957) Synthese basisch substituierter, analgetisch wirksamer Benzimidazol-Derivate. *Experientia* 13:400–401. <https://doi.org/10.1007/BF02161116>
- Hunger A, Kebrle J, Rossi A, Hoffmann K (1960a) Benzimidazol-Derivate und verwandte Heterocyclen II. Synthese von 1-Aminoalkyl-2-benzyl-benzimidazolen. *Helvetica Chimica Acta* 43:800–809. <https://doi.org/10.1002/hlca.19600430323>
- Hunger A, Kebrle J, Rossi A, Hoffmann K (1960b) Benzimidazol-Derivate und verwandte Heterocyclen III. Synthese von 1-Aminoalkyl-2-benzyl-nitro-benzimidazolen. *Helvetica Chimica Acta* 43:1032–1046. <https://doi.org/10.1002/hlca.19600430412>
- Hunger A, Kebrle J, Rossi A, Hoffmann K (1960c) Benzimidazol-Derivate und verwandte Heterocyclen VI. Synthese von Phenyl-[1-aminoalkyl-benzimidazolyl-(2)]-essigsäureestern und -amiden. *Helvetica Chimica Acta* 43:1727–1733. <https://doi.org/10.1002/hlca.19600430634>
- Krotulski AJ, Manini A, Calello D, et al (2021a) *N*-piperidinyl etonitazene. https://www.npsdiscovery.org/wp-content/uploads/2021/11/N-Piperidinyl-Etonitazene_112221_ToxicologyAnalyticalReport.pdf?mc_cid=09d08f4c2f&mc_eid=UNIQID
- Krotulski AJ, Papsun DM, Kacinko SL, Logan BK (2020) Isotonitazene Quantitation and Metabolite Discovery in Authentic Forensic Casework. *Journal of Analytical Toxicology* 44:521–530. <https://doi.org/10.1093/jat/bkaa016>
- Krotulski AJ, Papsun DM, Walton SE, Logan BK (2021b) Metonitazene in the United States—Forensic toxicology assessment of a potent new synthetic opioid using liquid chromatography mass spectrometry. *Drug Test Anal* 1–15. <https://doi.org/10.1002/dta.3115>
- Mardal M, Andreasen MF, Mollerup CB, et al (2019) HighResNPS.com: An Online Crowd-Sourced HR-MS Database for Suspect and Non-targeted Screening of New Psychoactive Substances. *Journal of Analytical Toxicology* 43:520–527. <https://doi.org/10.1093/jat/bkz030>
- Morris H (2009) Synthetic opioids: the most addictive drugs in the world. In: *Vice*. <https://www.vice.com/en/article/9bdymy/hamiltons-pharmacopeia-804-v16n4>. Accessed 26 Oct 2020

- Nothias L-F, Petras D, Schmid R, et al (2020) Feature-based molecular networking in the GNPS analysis environment. *Nat Methods* 17:905–908.
<https://doi.org/10.1038/s41592-020-0933-6>
- Ortiz de Montellano PR, Nelson SD (2011) Rearrangement reactions catalyzed by cytochrome P450s. *Archives of Biochemistry and Biophysics* 507:95–110.
<https://doi.org/10.1016/j.abb.2010.10.016>
- Pluskal T, Castillo S, Villar-Briones A, Orešič M (2010) MZmine 2: Modular framework for processing, visualizing, and analyzing mass spectrometry-based molecular profile data. *BMC Bioinformatics* 11:395. <https://doi.org/10.1186/1471-2105-11-395>
- Pottie E, Tosh DK, Gao Z-G, et al (2020) Assessment of biased agonism at the A₃ adenosine receptor using β -arrestin and miniG_{ai} recruitment assays. *Biochemical Pharmacology* 177:113934. <https://doi.org/10.1016/j.bcp.2020.113934>
- Pöyhiä R, Kalso EA (1992) Antinociceptive Effects and Central Nervous System Depression Caused by Oxycodone and Morphine in Rats. *Pharmacology & Toxicology* 70:125–130. <https://doi.org/10.1111/j.1600-0773.1992.tb00441.x>
- Rawls SM, Benamar K (2011) Effects of opioids cannabinoids and vanilloids on body temperature. *Front Biosci* S3:822–845. <https://doi.org/10.2741/s190>
- Reavy P (2003) Utah case of potent drug is U.S. first. In: *Deseret News*.
<https://www.deseret.com/2003/6/3/19726293/utah-case-of-potent-drug-is-u-s-first>. Accessed 26 Oct 2020
- Sharma KK, Hales TG, Rao VJ, et al (2019) The search for the “next” euphoric non-fentanyl novel synthetic opioids on the illicit drugs market: current status and horizon scanning. *Forensic Toxicol* 37:1–16. <https://doi.org/10.1007/s11419-018-0454-5>
- Sorokin VI (1999) Illegal synthesis of etonitazene. *Journal of the Clandestine Laboratory Investigating Chemists Association* 9:20
- Sorokin VI, Ponkratov KV, Drozdov MA (1999) Etonitazene encountered in Moscow. *Microgram* 32:239–244
- Taracha E, Mierzejewski P, Lehner M, et al (2009) Stress-opioid interactions: a comparison of morphine and methadone. *Pharmacological Reports* 61:424–435.
[https://doi.org/10.1016/S1734-1140\(09\)70083-0](https://doi.org/10.1016/S1734-1140(09)70083-0)
- Truver MT, Smith CR, Garibay N, et al (2020) Pharmacodynamics and pharmacokinetics of the novel synthetic opioid, U-47700, in male rats. *Neuropharmacology* 177:108195. <https://doi.org/10.1016/j.neuropharm.2020.108195>
- Ujváry I, Christie R, Evans-Brown M, et al (2021) DARK Classics in Chemical Neuroscience: Etonitazene and Related Benzimidazoles. *ACS Chemical Neuroscience* 12:1072–1092. <https://doi.org/10.1021/acscchemneuro.1c00037>

- UNODC (2020) The growing complexity of the opioid crisis. Global SMART Update, Volume 24. Vienna
- UNODC (2021) CND Decision on international control of isotonitazene enters into force. In: <https://www.unodc.org/LSS/announcement/Details/65247392-26c7-4446-a2b6-270226103036>. Accessed 10 Jun 2021
- Vandeputte MM, Krotulski AJ, Papsun DM, et al (2021a) The rise and fall of isotonitazene and brophrine: two recent stars in the synthetic opioid firmament. *Journal of Analytical Toxicology* bkab082. <https://doi.org/10.1093/jat/bkab082>
- Vandeputte MM, Van Uytfanghe K, Layle NK, et al (2021b) Synthesis, chemical characterization, and μ -opioid receptor activity assessment of the emerging group of “nitazene” 2-benzylbenzimidazole synthetic opioids. *ACS Chem Neurosci* 12:1241–1251. <https://doi.org/10.1021/acchemneuro.1c00064>
- Vasudevan L, Vandeputte MM, Deventer M, et al (2020) Assessment of structure-activity relationships and biased agonism at the Mu opioid receptor of novel synthetic opioids using a novel, stable bio-assay platform. *Biochemical Pharmacology* 177:113910. <https://doi.org/10.1016/j.bcp.2020.113910>
- Verougstraete N, Vandeputte MM, Lyphout C, et al (2020) First report on brophrine: the next opioid on the deadly new psychoactive substances’ horizon? *Journal of Analytical Toxicology* 44:937–946. <https://doi.org/10.1093/jat/bkaa094>
- Volpe DA, McMahon Tobin GA, Mellon RD, et al (2011) Uniform assessment and ranking of opioid μ receptor binding constants for selected opioid drugs. *Regul Toxicol Pharmacol* 59:385–390. <https://doi.org/10.1016/j.yrtph.2010.12.007>
- Walton SE, Krotulski AJ, Logan BK (2021) A Forward-Thinking Approach to Addressing the New Synthetic Opioid 2-Benzylbenzimidazole Nitazene Analogs by Liquid Chromatography–Tandem Quadrupole Mass Spectrometry (LC–QQQ–MS). *Journal of Analytical Toxicology* bkab117. <https://doi.org/10.1093/jat/bkab117>
- Wang M, Carver JJ, Phelan VV, et al (2016) Sharing and community curation of mass spectrometry data with Global Natural Products Social Molecular Networking. *Nat Biotechnol* 34:828–837. <https://doi.org/10.1038/nbt.3597>
- Williams JT, Ingram SL, Henderson G, et al (2013) Regulation of μ -Opioid Receptors: Desensitization, Phosphorylation, Internalization, and Tolerance. *Pharmacol Rev* 65:223–254. <https://doi.org/10.1124/pr.112.005942>
- Wong B, Perkins MW, Tressler J, et al (2017) Effects of inhaled aerosolized carfentanil on real-time physiological responses in mice: a preliminary evaluation of naloxone. *Inhalation Toxicology* 29:65–74. <https://doi.org/10.1080/08958378.2017.1282065>

Supplementary Information

A.



B.

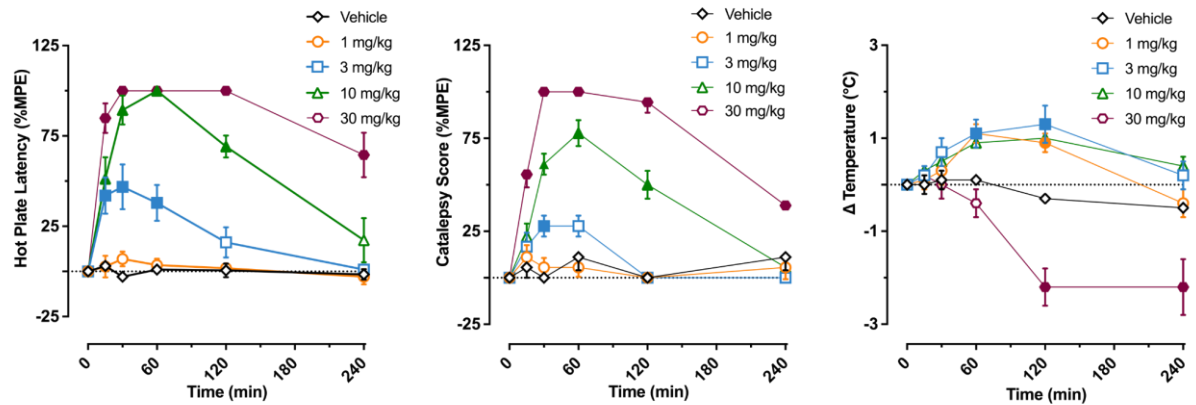


Figure S1. Time course of pharmacodynamic effects induced by subcutaneous saline (vehicle, 1 mL/kg), fentanyl (A) (0.003, 0.010, 0.030, 0.10 mg/kg) or morphine (B) (1, 3, 10, 30 mg/kg) in male rats. Hot plate latency, catalepsy score, and body temperature are depicted as mean \pm SEM for $n = 6$ rats per dose group. Hot plate latency and catalepsy scores are presented as a percent of maximum possible effect (%MPE), whereas temperature data are expressed as change from baseline (Δ temperature in $^{\circ}$ C). Filled symbols indicate significant differences as compared to the vehicle-treated group at a given time point ($p < 0.05$, Tukey's).